P-ISSN: 2798-1134 | E-ISSN: 2797-3549 | DOI: 10.52562/injoes.2025.1250

Indonesian Journal of Earth Sciences

https://journal.moripublishing.com/index.php/injoes

| Research Article |

Geotectonics and Exploration of Gold Mineralization in the Kushaka-Kusheriki Schist Belt North-Central Nigeria

Cyril C. Okpoli[1]*, Sunday O. Idakwo[2], Oladele Olaniyan[3], Promise E. Chidi[1]

[1]Department of Earth Sciences, Faculty of Science, AdekunleAjasin University, PMB 1, Akungba-Akoko, Ondo State, Nigeria
[2]Department of Geology and Mining, Faculty of Applied Science and Technology, Ibrahim Badamasi Babangida University, Lapai, Niger State, Nigeria
[3]Geodel integrated, Abuja, Nigeria
**Correspondence: cyril.okpoli@aaua.edu.ng*

Received: 16 July 2024 / Accepted: 16 December 2024 / Published: 14 April 2025

Abstract: The lack of systematic and organized development and exploration for gold and increasing demand for sustainable development goals has prompted the integrated geological, geophysical and geochemical surveys to characterize the gold mineralization at Owu part of the Kushaka-Kusheriki schist belt in North Central Nigeria. Previous studies concentrated on geology and geochemical studies with no emphasis on the use of integrated studies and state-of-the-art tools aimed at characterizing gold mineralization. Detailed geological mapping was carried out to determine the various rock types and their structural framework. Thirty- one (31) data were acquired using Proton Precession Magnetometer for geophysical survey to delineate their degree of magnetic susceptibility and dataset was enhanced using Fast Fourier Transforms (FFT). Inductively Coupled Plasma/Optical Emission Spectrometry (ICPOES), fire assay, multi-acid digestion with gravimetric method were carried out on rocks and soils to determine their geochemical signatures. Geologically, the study area consists of phyllite, mica schist, amphibole schist, phyllitic schist, biotite schist within schist shear zone. Structurally, granitic intrusions are observed in the NE-SW direction, parallel to the regional foliation of the rocks. Geophysical data were subjected to different forms of filtering, which showed high and low magnetic areas. The results reveal a distinct tectonic activity that led to shearing and fracturing, and subsequently gave rise to a structurally controlled mineralization pattern (i.e., NE-SW direction in the Pan African domain). ICPOES analysis yielded Au concentration of <0.2 – 201 ppm with 80% of the soil samples exceeding 2 ppm indicating their qualification as ores. The soil samples are enriched in W (1 – 241 ppm), Mo (1 – 19.8 ppm) but depleted in Sb (<5) and Ag (<2 ppm). Positive correlations between Au and Cu, Zn and Pb confirm that they are pathfinder elements for Au in the area. The geological and geophysical studies reveal structurally controlled mineralization; while the very low K/Ba (<0.01) suggests non- structurally controlled gold mineralization in sediments occasioned by dispersion of the metals. The integrated approach has proved effective in delineating gold mineralized zones, and is recommended for other related investigations.

Keywords: Structural, geochemical, geophysical, shear zone, pathfinder elements, Kushaka-Kusheriki schist belt

INTRODUCTION

Gold mining activities has been recognized as one of the exploration and exploitation endeavours that have positive impacts in the nation's economy by diversifying the economic base of Nigeria especially as it regards to the solid mineral resources (Lu et al., 2015; Adeyi & Babalola, 2017) Northcentral Nigeria has abundance of mineral resources which are: Tin –tantalum-niobum, pegmatites, lead-zinc sulphide, coal-lignite, talc, marble, gemstones, gold, columbite, cassiterite, fluorite, lithium, iron-ore, wolframite. Owu being part of Kushaka-Kusheriki schist belt has huge mining potential of gold deposit for the country. Previous studies have revealed the incidence of distributed metal concentrations in various schists, protobasins, veins, placers, etc of the nation (Smouni et al., 2010; Rasheed & Abdulgafar, 2014; Chouti et al., 2018). The economic development and growth of any nation rely highly on the abundance of mineral resources, that have wide applications to the economics of any country. Nevertheless, these economic minerals must be explored and exploited to harness its economics and viabilities for nations economic development (Moon et al., 2006).

Gold is found mostly in quartz veins, soil as placers (eluvial), and stream sediments (alluvial). Gold-bearing quartz veins can be found in metamorphosed rocks ranging from semipelitic to pelitic to

mafic in composition. Primary gold mineralization generates a unique pattern for exploration (chemical signature) in the overburden and nearby soil possibly through weathering processes. Weathering processes offer samples (soils and stream sediments) that yield data on local hidden mineralization. For the soil samples, the origin of the gold-bearing fluid was hypothesized and the residual soil is the geochemical sample that is frequently used to identify the location of concealed mineralization once a region of economic significance is localized (Siegel, 1974). Groundwater movement, deep within the earth causes a chemical reaction at the subsurface, resulting in an elemental distribution pattern (Darnley et. al., 1995). Most of these isolated elements (e.g., Cu, Ag, Zn, As, Bi, Pb, Sb, Hg, W, Mo. and Se) are useful marker for the occurrence of gold (Antweiler & Campbell, 1982; Oyediran et al., 2020). However, conventional approach and inappropriate use of hazardous substances like mercury, cyanide to leach gold out of the ore during antisanal mining and exploitation and indiscriminate disposal of gangue without sustainable management has been the practice for years. Furthermore, geochemical analyses are greatly challenging because of its cost ineffectiveness despites its wide significance (Rollinson, 2014; Scott et al., 2002; LeBoutillier, 2004; Clark et al., 1986).

Recent improvement in the analysis of geophysical data and enhancement transforms, have increased geophysical dataset resolution, so that very insidious changes in responses can be seen (Armstrong & Rodeghiero, 2006). More so, state of the art equipment is currently being utilized in fingerprinting the geochemical signatures for metallic ores.

Mapping mineralization potential is frontier work commonly completed during exploration projects to concentrate following exploration efforts on areas that show significant prospects and where spending time and resources will provide the most exceptional results (Davies et al.,2020). Integrated approach with appropriate instruments for mineral potential investigation in a frontier geologic setting of Kushaka-Kusheriki schist belt of northcentral Nigerian; is evaluated with aim to map the potential of gold mineralization of the schist belt in an unbiased and reliable manner, taking Geological, geophysical and geochemical methodologies into account. The study aimed to lower systematic ambiguities and improve understanding of the surface and subsurface geological control of mineralization using detailed geological, geophysical and geochemical mapping and data interpretation. Consequently, the present study comes with specific objectives of mapping the potentially mineralized alteration zones localities at Kushaka-Kusheriki schist belt and delineating the effective surface and subsurface structures controlling the mineralization at this area using integrated fieldwork geological, geophysical and geochemical approach supported and validated by state-of-the-art laboratory and computational analyses.

Numerous, previous related studies have been carried out in northcentral Nigeria (study area inclusive) for its mineralization potential. However, most of this research was conducted in pockets of the study area; for example, Andongma et al. (2021) studied the alteration zones favourable for gold mineralization within the Malumfashi schist belt. Arogundade et al. (2022) investigated some part of Zamfara mineralization potential using integrated geophysical data. Augie et al. (2023) evaluated the gold mineralization potential of some parts of the study area using magnetic datasets. Salawu et al. (2023) and Augie et al. (2023) employed the remotely sensed geophysical and magnetic datasets to delineate structures favourable for gold mineralization in the southern axis of the Zuru schist belt and Kebbi respectively. Usman & Ibrahim (2017) and Oke et al. (2014) carried out petrography and geochemistry of the rocks as well as mineralogical and geochemical characterization of gold within the Wonaka and Maru schist belts respectively. Sanusi & Amigun (2020) mapped structural and hydrothermal alteration studies associated with orogenic gold mineralization in part of Kushaka schist belt, North-central Nigeria, by employing aeromagnetic and aero-radiometric dataset. Despite all these studies, none of these studies have integrated holistically, geological, geophysical and geochemical approaches in data acquisitions and analyses.

However, this study assessed the geotectonics and mineralization potential of Kushaka-Kusheriki schist belt using integrated detailed geological, geophysical and geochemical methods. The study developed suitable exploration methods to evaluate and analysed the geotectonics and hydrothermal alteration zones promising for mineralization within the study area. The outcomes of this gold mineralization research study could promote significant interest in exploration and exploitation in Nigeria.

Site description and geological setting

The study area is surrounded by mountains giving it a lower elevation than the surrounding mountains which are located nearby. The area is relatively flat, but the topography undulates gently with some valleys and floodplains. High elevated outcrops are not dominant in the area. The rocks in

the study area are mostly deformed and weathered. Most of the resistant rocks are observed and some outcropped along stream channels.

The study area is located in north-eastern part of Minna, in Owu village, Kuta local government area, Niger state, north-central Nigeria with Longitude 6.7093°E and Latitude 9.8714°N (Fig. 1). The study area lies within the Kushaka- Kusheriki schist belt of the NW, Nigeria basement complex and metallogeny province of Nigeria, the area has been interrupted by large mass of granitic rocks that led to broad migmatization of metasedimentary and metavolcanic rocks carrying considerable gold mineralization (Garba, 2002). Geology of the study area comprises crystalline rocks (Fig. 2) that have been divided into three categories analogous to that of Nigeria basement complex, which are:

1. A basement unit involving gneisses and migmatite with relicts of supracrustal rocks.
2. North-south trending schist belts composed of medium-to low grade supracrustal cover.
3. Intrusive granitic rocks (Older Granite Suite) which intrude both the gneiss, migmatite and the low-grade schist belt.

Kusheriki – Minna region belts comprise Kushaka, Birnin Gwari and Ushama schist belts, and are representative of the geology of NW schist belt of Nigeria (Ajibade, 1980; Sanusi & Amigun, 2020).

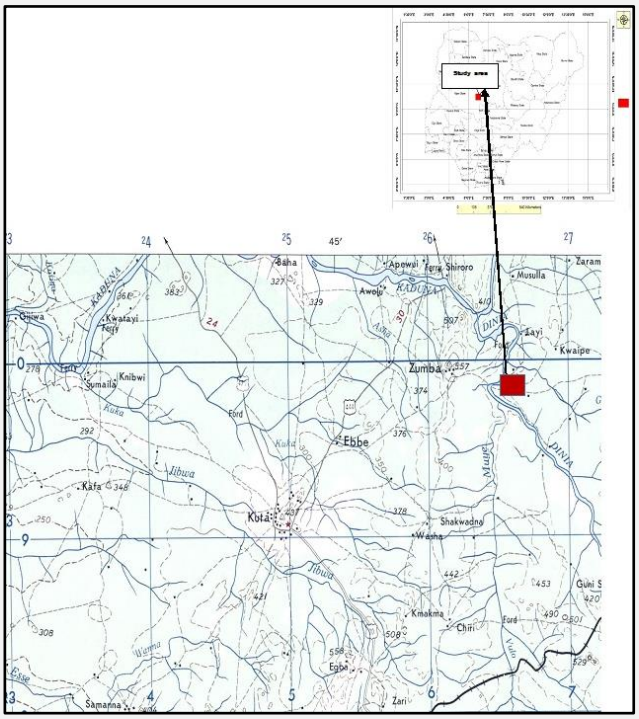

Figure 1. Location map of the study area (red box).

The most predominant soil type is the ferruginous tropical soils which are basically derived from the Basement Complex rocks, as well as from old sedimentary rocks. The exploration area is located about 30 km from Minna in Niger State. From Abuja, the site is easily accessible via double carriage road through Minna (Fig. 1).

MATERIAL & METHODS

Geological Survey

The geological mapping of the study area involves taking strike and dip direction of the several rocks types. Owu area is part of the Kushaka-Kusheriki shear zone and have undergone several episodes of orogenies. Most of the rock types were identified to be metamorphic rocks. Global positioning system (GPS) was used to take the longitude, latitude and elevation of the study area. The rocks were identified to be schist, phyllite, amphibole schist, biotite schist, gneiss, granite gneiss, quartz rubbles. Primary mineralization in Nigeria is generally lithologically and structurally restricted (Ajakaiye et. al., 1991; Sanusi & Amigun, 2020). The structures observed in the study area consist of faults, fractures, micro-folds, shear zones (lineaments), pegmatites, quartz and quartzite vein. Table 1 below gives a descriptive study of the geological survey carried out in the study area.

Table 1. Descriptive study of the geological survey carried out in the study area

Location id	Longitude (e)			Latitude (n)			Elevation (m)	Rock type	Lithology	Colour	Texture	Strike	Dip/ Direction	Structures	Observation
L1	6	40	29.7	9	40	59.9	322	Metamorphic	Phyllitic schist	Grey- light grey	Fine-medium	16	53/E		Parrallel sets of quartz veins embedded within the rock
L1B	6	40	29.7	9	40	59.9	322		Quartz body/ rubbles	Brownish	Medium-coarse				An altered quartz body at 7-m eastward of location 1
L2	6	40	19	9	41	51.4	340	Metamorphic	Schist	Grey- light grey	Fine-medium				Highly weathered exposure
L3	6	40	11.3	9	41	11.3	363	Metamorphic	Schist	Grey-dark grey	Fine-medium	10	82/E		Hilly exposure trending n-s with quartz veins & rubbles
L3B	6	40	7	9	41	46.6	368		Quartz rubbles	Brown-reddish	Medium-coarse				The dimension of the quartz rubbles is about 20m by 10m
L3C	6	40	3.6	9	41	45.7	352	Metamorphic	Biotite schist	Dark-grey	Fine-medium				
L4	6	40	3.4	9	41	42.4	361	Metamorphic	Phyllitic schist	Dark-light grey	Fine-medium	5	59/E		A thin quartz veins embedded within the rock and q/r
L5	6	39	42.6	9	41	38	334	Metamorphic	Schist	Dark-grey	Fine-medium	40	64/E	Micro fold	Quartz veins observed & lots of quartz rubbles
L5B	6	39	40	9	41	33.6	322	Metamorphic	Schist	Dark-grey	Fine-medium	22	66/E		Quartz veins with strike of 19 & thickness of 16cm
L6	6	39	18.3	9	41	31.2	335	Metamorphic	Granite-gneiss	Greyish	Medium	38	59/E		It occurs in bouldery form with lots of quartz veins
L7	6	39	15	9	41	38.3	320	Metamorphic	Schist	Light-grey	Fine-medium	12	E		Stream sediment are being packed for gold panning
L8	6	39	51.4	9	42	18.2	321	Metamorphic	Amphibole schist /gneiss	Greenish/light & dark band	Fine-medium	51	40/E(SE)		Two lithologies (amphibole schist & gneiss) & quartz r.
L9	6	41	36.2	9	42	53.2	368	Metamorphic	Schist		Fine-medium	166	E		Signs of mineralization on quartz rubbles
L9B	6	41	34.5	9	42	52.1	371	Metamorphic	Phyllite	Light-grey	Fine-medium	188	82/E		Quartz veins in concordant with the country rock
L10	6	41	37.2	9	42	57.2	367	Metamorphic	Phyllite	Light-grey	Medium-coarse	28	50/W	Fracture	Quartz veins of about 12cm thick and veinlet(1cmby10cm)
L11	6	41	30	9	42	53	365	Metamorphic	Phyllite	Brownish- grey	Fine-medium	9	48/E		Upland bouldery exposure with lots quartz vein
L12	6	41	48.8	9	42	38.2	353		Quartz body/veins	Whitish/milky	Fine-medium	42			Parrallel sets of quartz veins with a width of about 60m
L13	6	41	41.7	9	42	25.2	359		Quartz rubbles	Whitish/milky	Fine				A gentle uphill of quartz rubbles
L14	6	41	51.6	9	42	19.8	356		Quartz body	Whitish/milky	Fine	22	46/E	Fracture	Bouldery exposure of quartz body of about(50mby30m)
L15	6	41	35.7	9	42	15.5	357		Quartz body	Whitish/milky	Fine	128		Fracture	Upland of quartz body in insitu & quartz rubbles
L16	6	41	30.8	9	42	7.7	328	Metamorphic	Phyllitic schist	Light-grey	Fine-medium	38	68/E		The exposure is highly foliated with some quartz veins
L17	6	41	27.7	9	41	50.3	320	Metamorphic	Phyllitic schist	Grey-dark	Fine-medium	38	68/E		The exposure is dipping eastward & trending ne-sw
L18	6	41	14.6	9	41	59	328	Metamorphic	Phyllitic schist	Grey-light grey	Fine-medium	11	40/E		Quartz veins of about 10cm by 50cm & some thin veinlet
L19	6	41	6.6	9	41	53.4	340		Quartz body	Whitish/milky	Fine			Fracture	An upland exposure quartz body in bouldery form
L20	6	40	32.4	9	42	0	325	Metamorphic	Phyllitic schist	Grey	Fine-medium	180			The exposure is along a stream channel
L21	6	40	41.4	9	42	13.7	331	Metamorphic	Phyllite	Grey	Fine	10	68/W	Fracture	A highly jointed exposure with a lots of quartz veins
L22	6	41	23.2	9	42	46.6	355	Metamorphic	Granite-gneiss	Light-grey	Medium-coarse	19		Fracture	Hilly exposure with several boulders & thin quartz veins
L22B	6	41	28.6	9	42	51.2	357	Metamorphic	Granite-gneiss	Dark-grey	Medium-coarse	20		Fracture	The exposure has a quartz veins & a lots of quartz r.
L23	6	41	31.9	9	42	52.7	364	Metamorphic	Schist	Grey	Medium-coarse	22			A contact btw the schist & granite gneiss
L24	6	42	0	9	41	24	331	Metamorphic	Phyllitic schist	Grey	Fine	32	28/E	Microfold	It occurs along a stream & it's becoming gradational
L25	6	41	51.5	9	41	27	335		Quartz veins	Reddish-brown	Fine-medium	140			An occurrence of quartz veins with sign of alteration
L26	6	41	15.2	9	41	28.1	338		Quartz rubbles	Reddish-brown	Fine-medium				A hilly exposure of quartz rubbles
L26B	6	41	4.3	9	41	29	332		Quartz rubbles	Whitish/milky	Fine				A fixed spread of quartz rubbles of about 150m
L27	6	41	15.3	9	41	15.6	327	Metamorphic	Phyllitic schist	Grey-light grey	Fine-medium	54	26/E		A flat exposure that is highly weathered
L28	6	41	28	9	41	10	326	Metamorphic	Phyllite	Grey	Fine-medium	54	32/E		A very small exposure
L29	6	40	35.9	9	42	34.8	311		Quartz rubbles	Whitish-brownish	Fine-medium				A spread of quartz rubble on gentle upland
L30	6	40	23	9	41	31.8	329	Metamorphic	Amphibole schist	Greenish-grey	Fine-medium				A small flat exposure
L31	6	40	14.8	9	41	28.8	319	Metamorphic	Amphibole schist	Greenish-grey	Fine-medium	20	41/E		A well foliated body along a stream channel with q.r
L32	6	40	4.3	9	41	9.1	313	Abandoned gold panning pit							The pit is about 5m deep with no traceable vein
L33	6	40	6.9	9	41	16.1	318		Quartz rubbles	Whitish-brownish	Fine-medium				Quartz rubbles close to a first order stream
L33B	6	40	8.2	9	41	17.1	318	Proposed panning point							First order stream running south to river mauna/ose
L34	6	40	8.6	9	41	18	317	Metamorphic	Schist	Grey	Fine-medium	4	70/E		Quartz veins embedded within the host rock

Geophysical (Magnetic Survey)

The method of geophysical survey was structured for this investigation to capture the common trends of gold mineralization in the area. Ground magnetic survey was carried out in the study area to search and delineate the mineral bearing ores. Figure 3 shows the plot of survey pattern adopted during the ground magnetic survey of the study area. The magnetic data was collected along thirty-one (31) profile lines of 4 km long east-west at an interval of 100 m. The ground magnetic mapping is an aid to geological, geotectonic and structural study of rocks (Oyeniyi et al. 2016). The data was transformed to Total Magnetic Intensity (TMI) and was later reduce to the equator (RTE) The magnetic inclination (0.36) and magnetic declination (-1.83) were used on the International Geomagnetic Reference Field (IGRF) 2016 on the magnetic calculator to generate RTE. The regional-residual separation was carried out to produce the residual grid using the least squares polynomial fitting method. The result was later subjected to filtering techniques like second vertical derivative to enhance the structural dynamics (Gibert & Galdeano, 1985).

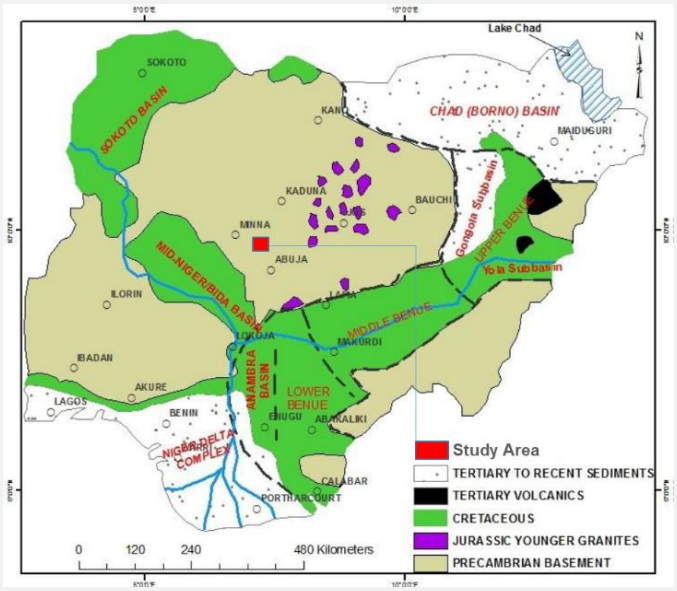

Figure 2. Geology map of Nigeria indicating the study area (Obaje, 2009).

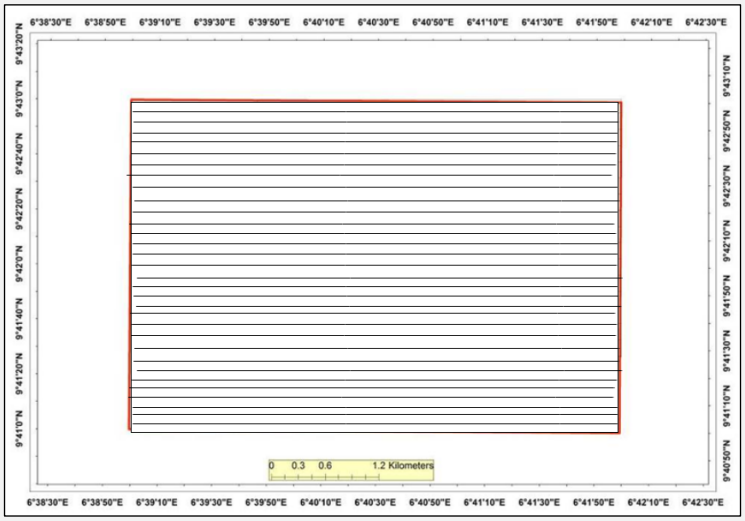

Figure 3. Profile lines of ground magnetic surveyed area.

The survey was designed to cover the gold fire assay anomalous locations delineated from the geochemical sampling, while the survey direction was designed to traverse the mapped NE regional

trend of outcropping geological structures. The acquired ground magnetic data was downloaded into the survey database and checked for quality control, spike elimination and filtering. The data was corrected for diurnal variation and gridded accordingly (Reeves et al., 1998). The merged magnetic dataset was micro-levelled using Minty approach (Minty, 1991) to remove directional noises along and across the survey line. The study area magnetic field varies from 29,448 nT and 30, 320 nT.

Geochemical Surveys

The target areas were sampled on a grid spacing of 200m by 100m in UTM (Universal Traverse Mercator) coordinate system. The sampling profile lines run in the east-west direction, traversing across major lineaments and mapped geologic trends. The selected target areas were delineated into sections A, B and C (Figs. 4 and 5). Samples were taken at a uniform depth of 25cm below the 'A' horizon where no organic structure (decomposing plant or animal tissue) were observed. Samples of about 4-6 kg of soil from each location were bagged in clean, properly labelled plastic bags and the soil type noted. Some samples were panned, the panned concentrate recovered are mostly heavy concentrates and some gold specks which was then bagged in a smaller Ziploc bag and labelled accordingly. The soils and rock samples were analysed in SGS South Africa (Pty) (Ltd), Zuurbekom road, Randfontein, South Africa. Out of the 401 samples analyzed at the SGS laboratories in South Africa using Fire assay for gold and multi-acid digestion methods while two hundred and two (202) soil samples were weighed and dried for gravimetric analysis (Skoog et al., 1996; Odokuma-Alonge & John, 2013). Inductively coupled plasma/optical emission spectrometry (ICP/OES) was used for metal and trace elements matrix determination which is hinged on radiofrequency (RF) spontaneous emission of photons from atoms and ions. Most of the samples were multi-acid digested to solution (coded: ICP-40B), and introduced into induced RF argon plasma and several nebulizers. At plasma excitation state the mist was energized and vaporized. Then the plasma was viewed and collected in axial array via lens, and imaged onto the entrance slit of a wavelength selection device. Fire assay and ICP-OES methods determine the gold lead fusion and silver. The bulk chemical analyses of major elements (Ti, Al, Fe, P, Mn, Mg, Ca, Na, K, P) and trace elements (>1 ppm; Au, Ag, Ba, Be, Bi, Ce, Co, Cr, Cu, La, Li, Mo, Ni, Pb, Sb, Sc, Sn, Sr, V, W, Y, Zn, Zr) was determined using ICP/OES.

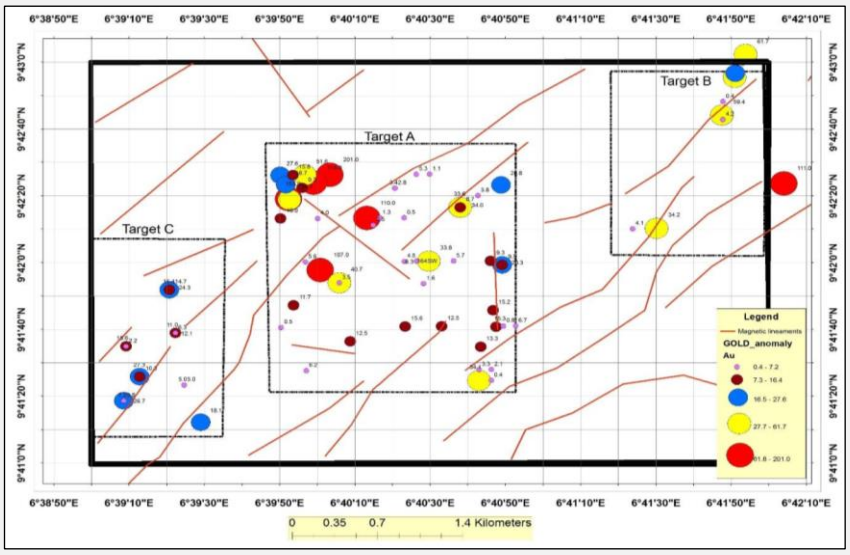

Figure 4. Geochemical sampling target points in section A, B and C.

In this investigation, the Upper Continental Crust (UCC) value of the elements (Taylor & McLennan, 1995) were used as baseline or background values.

$$Enrichment\ ratio\ (ER) = \frac{Cn}{Bn} \quad (1)$$

C_n = Element measured in the soil samples and B_n = Background or baseline concentration (UCC values of the element was used).

Figure 5. (A) Soil dug up for sampling, (B) Panning done by locals in the stream. (C) Recovered panned concentrates contain some gold specks, heavy metals and sand. The samples were then bagged, ready to be transported to the laboratory for analysis.

RESULTS

Geological

Field relationship/occurrence

The area covered by the study is generally underlain by quartz rubbles/ridges, mica schist, phyllite (Figs. 5, 6 and 8). There is also the intrusion of granitic-gneiss into the host rock trending NE – SW (Fig. 6). Multiple quartz veins are also observed in phyllitic host rock at the north-eastern part of the study area, and this indicates an area of interest as gold usually occurs in quartz veins (Fig. 6). The various outcrops trend NE-SW. Another pointer to gold mineralization in the study area is associated with observation of identified artisanal working (streams and pits) in the area mainly along the south-western part of the study area from where panned samples observed gold specks (Fig. 5). Seventy-six (76) samples returned gold assay values that ranged between 0.4ppm and 201 ppm in soil samples, the 76 samples that ranged above the 0.4 ppm (set threshold) were plotted on geological and magnetic maps to demonstrate the likely spatial distribution and anomalous relationship with the interpreted geological units, contacts and structures (Usman & Ibrahim, 2017; Sanusi & Amigun, 2020; Salawu et al., 2023).

Phyllite: A particular kind of metamorphic rock called phyllite is created when slate undergoes additional metamorphism. Its colour varies from light greyish to greenish, and its fine-grained texture and unique glossy sheen or luster are caused by the parallel alignment of small mica crystals. They are made of mica, quartz, and chlorite and are created at temperatures and pressures that range from low to moderate. Phyllite is an intermediate stage of shale/mudstone metamorphism that is between slate and schist on the metamorphic grading spectrum (Usman & Ibrahim, 2017; Sanusi & Amigun, 2020) Phyllite were observed with strike of 28, dipping 50oW and fractured with quartz veins of about 12cm thick and veinlet (1cm by 10cm) (Fig. 6 and 8).

Figure 6. (a) Phyllite, L28, (b-c) L10, (d-g) phyllite rock with quartz veins of about 12cm thick and veinlet (1cm by 10cm) L21, (h) L23, Schist.

Quartz body/veins: Common geological structures known as quartz veins or quartz bodies are formed when the silicate mineral quartz crystallizes in rock fissures. These veins originate from silica-rich fluids that seep into host rock fissures and, in some cases, deposit quartz as they cool or alter chemically. Hydrothermal activity, which is the passage of hot, mineral-rich water through the Earth's crust, is the process that created quartz veins. As this fluid cools, it may deposit minerals like quartz through fissures or cracks in rocks. As quartz precipitates out of the fluid, it fills up the fractures and forms a vein. Depending on the unique geochemical conditions of schist belts, quartz veins are typically associated with other minerals, such as gold with pyrite, arsenopyrite, or other sulfide minerals; silver, copper, lead, zinc, and sulphide minerals like pyrite (fool's gold), chalcopyrite, galena, and sphalerite (Usman & Ibrahim, 2017; Sanusi & Amigun, 2020) An upland exposure quartz body in boulder form was observed during the mapping. A quartz vein with a width of about 60m and strike of 40m was also observed, altered, concordant to their host rock and some discordant (Figs. 7 and 10).

Figure 7. (A) Quartz veins/bodies; (B) Quartz body that has been broken down; (C) Quartz rubbles; (D) shows pebble to boulder sized quartz veins; (E) Large boulder of quartz; (F) shows quartz body in boulder.

Granite gneiss: One kind of gneiss, a high-grade metamorphic rock, is granite gneiss. It is created when granite, an igneous rock, goes through severe regional metamorphism, typically in the Earth's crust, amid extreme pressure and temperature fluctuations. The outcome is a gneiss texture that is characterized by banding or foliation, which is caused by the alignment of minerals under directed pressure. Quartz, biotite/muscovite, and potassic-feldspar make up their composition. Whereas quartz and feldspar make up the lighter bands, biotite and hornblende make up the darker bands. Greyish medium to coarse grained granite – gneiss was found at different locations within the study area, occurring in boulder for with lots of quartz veins. Prominent, among them was the granite gneiss with a strike of 38 and dipping at 59o to the East (Fig. 10). The granites, granite gneiss observed in the study area witnessed polyclic deformation processes (Rahaman et al., 1983; Usman & Ibrahim, 2017; Sanusi & Amigun, 2020).

Schist/amphibolite schist: Schist/Amphibolite schist is a metamorphic rock with medium to coarse grains. It is distinguished by its well-developed foliation, which is the ability of micas and other platy minerals to split into thin, parallel layers. On the other hand, amphibolite schist is rich in amphibole minerals, especially hornblende, which gives it unique mineralogical and textural properties. Below is an explanation of each: Amphibolite schist is generated by metamorphism, which permits the mineral to grow larger and align in a schistose texture. Schist is formed under higher pressure and temperature of shale/mudstone. Due to the predominance of platy minerals like mica, schist is typically recognized for

its glossy, layered texture. In contrast, amphibolite schist is harder, darker, and has a more massive structure because of the presence of amphiboles, giving it a more blocky or difficult to split appearance than schists rich in mica. During the mapping exercise, schist was found at various locations, in some cases occurring as amphibolite, phyllite, or biotite schist with quartz veins or quartz rubbles embedded in it (Usman & Ibrahim, 2017; Sanusi & Amigun, 2020) They are generally light to dark grey in colour, fine to medium grained with the general trend being north to south (Figs. 9 and 10).

Figure 8. A–B: Granite gneiss with fractures observed; C–E: Low lying exposure of granite gneiss; F-G: Granite–Gneiss rubbles.

Figure 9. Pictures of amphibole schist, biotite schist observed at different locations during the geologic mapping of the study area (a-b) Location 30; (c-d) Location 31.

Geophysical

Integration of geophysical and geochemical surveys

Figure 11 revealed the plot of gold concentration with respect to depth. We observed that at target zone A, samples were acquired from four pits with depths of 0.5 m, 1 m, 1.5 m and 2 m as plotted in Fig. 11, indicating that average gold assay from the four pits was 17.3 ppm. Target B illustrated where stream sediments were sampled upstream to the source of the stream uphill and fire assay detected up to 61.7 ppm of gold while Target C was soil samples which were obtained randomly in the located pits.

Plot UAPIT27 revealed presence of UAPIT27C which has gold concentration 20.3 ppm at depth of 1-1.5 m while UAPIT27A has gold concentration of 9.5ppm at depth of 0-0.5 m. Chart UAPIT16 showed UAPIT16O with record of 3.4 ppm at depth of 1.5-2 m while UAPIT16C has gold concentration of 2.8 ppm at depth of 1- 1.5 m. Plot UAPIT14 illustrated plot of UAPIT14C having gold concentration of 3.5 ppm at depths of 1- 1.5 m, while UAPIT148 recorded gold concentration of 40.7 ppm at depths of 0.5-1 m. UAPIT17 chart revealed UAPIT17A recorded gold concentration of 8.7 ppm at depths of 0-

0.5 m, , UAPIT17B recorded gold concentration of 31.6 ppm at depths of 0.5-1 m while UAPIT17C witnessed gold concentration of 34 ppm at depths of 1- 1.5 m. All the plots are clearly revealed in targets A, which are shown in Figs. 12 and 13.

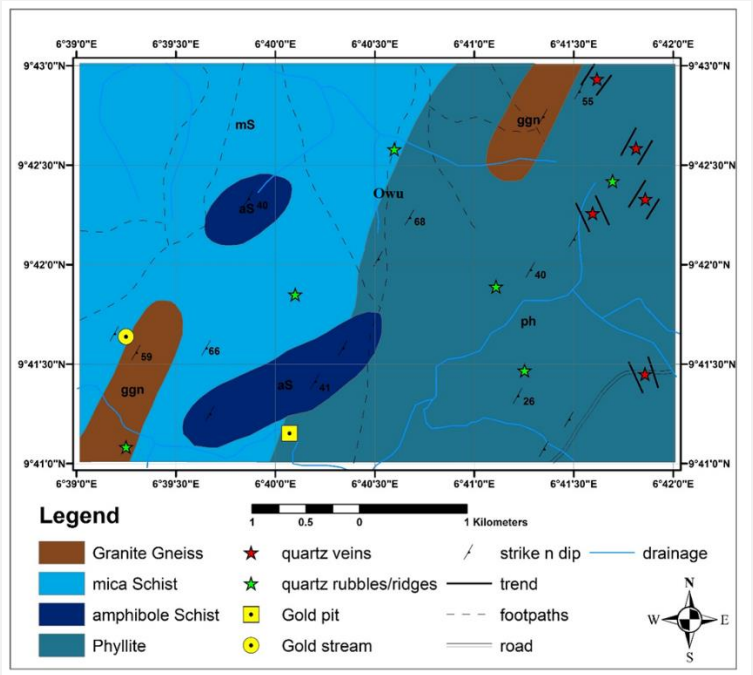

Figure 10. Detailed geological map of Owu showing major rock types and suspected gold deposits along structural veins.

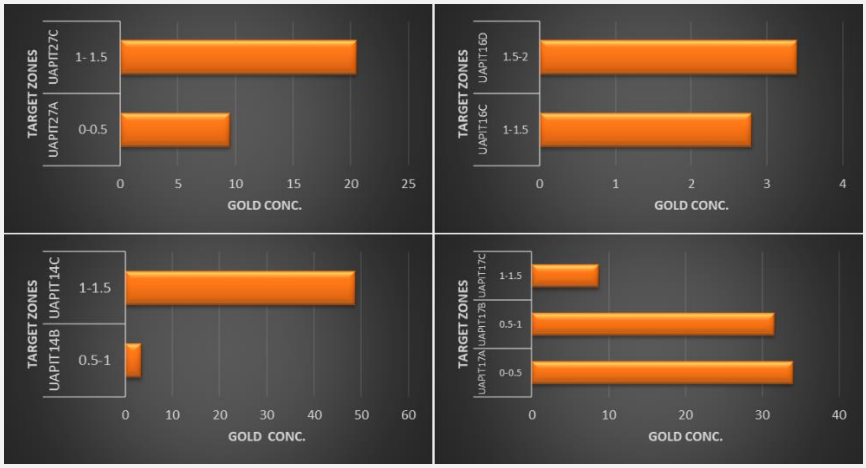

Figure 11. Plot of Gold concentration with depth.

Zone A has anomalous gold values on both the ridge and the base of the ridge. The Locations fall on the higher elevation near the peak in the south-western section of the study area (Figs. 12, 13 and 14). As gold cannot be transported up the slope by water, alluvial gold is acquired from the primary upper elevation, placer gold mineralization in the weathered zone indicates fresh primary host rock at farther depth (Fig. 14).

Zone C is located at lower elevation of the sheared belt, anomalous gold values at shallow depths suggested transportation of materials owed to area gradient (Figs. 12 and 13).

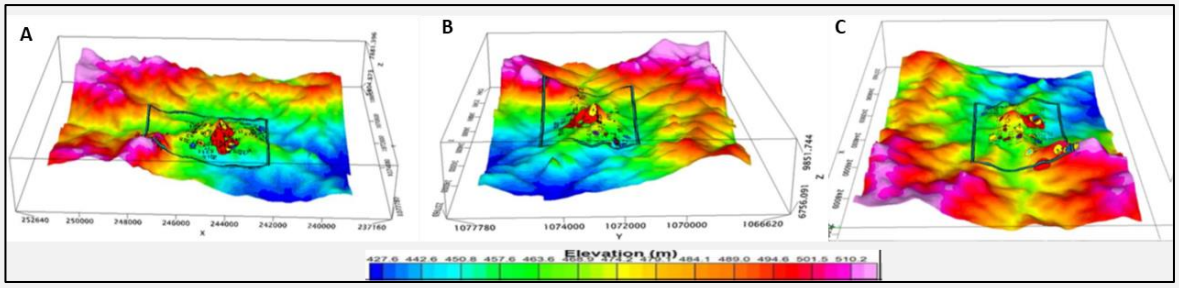

Figure 12. Dimensional elevation model of the project A, B and C pointing south, east and west Respectively.

Regional magnetic map superimposed with geochemical survey

Target A at the Centre of the survey area had gold fire assay values ranging from 0.4 – 201 ppm, Duplicate samples were collected at some locations where gold specks were recovered from during the sampling.

A cluster of anomalous values occurred in the NW of the area, while a series of gold anomalous (up to 110 ppm) occurred along the NW trending shear zone (Fig. 13). Target B samples were stream sediments sampled upstream to its source uphill, fire assay detected up to 61.7 ppm of gold while at target zone C soil samples were obtained from seven randomly located pits.

Anomalous gold values up to 27.3 ppm were obtained from the panned concentrates along the corridor of NE magnetic trend interpreted as the shear zone. The near surface gold occurrence is thought to be alluvial gold deposit due to the drainage pattern and gradient of the area. Notwithstanding, gold occurrence in shallow pits along the shear zone, could be indicative of alluvial type of deposit and sulphide mineralization at depth (Fig. 13).

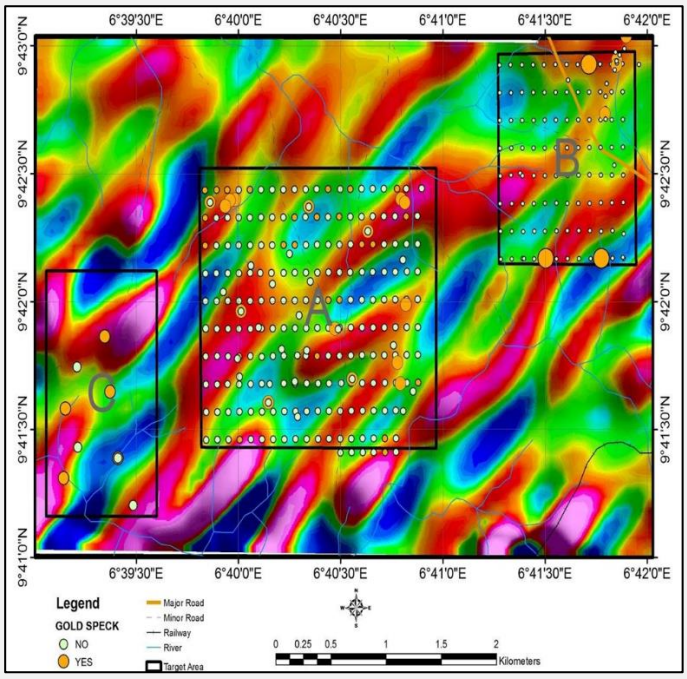

Figure 13. Sampling points within target area superimposed in magnetic map.

Anomalous gold assay locations were plotted on the regional magnetic map to relate the anomalous locations with magnetic structures indicated that the gold concentrations occur within a regional NE sheared zone, part of which appeared to have been folded and faulted. Target zone A is more related to a NW trending deformed structure (Fig. 14). The north-west sheared zone where most target A zone occurred has lots of deformation and the NW trend is associated with the Kibaran orogeny

The north-east sheared zone has undergone series of deformation in the Kushaka-Kusheriki schist belt. This also indicate that the study area has undergone several orogenies. The north-east sheared zone is associated with the Pan-African orogeny which happens to be the last episode in the study area (Okpoli & Oladunjoye, 2017).

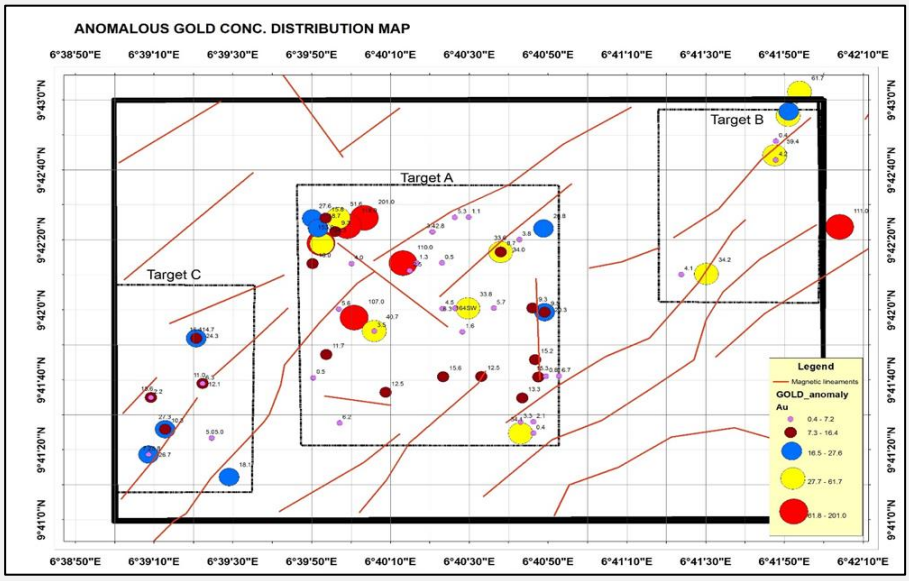

Figure 14. Map of the target zone A, B and C on the interpreted magnetic lineaments.

Total magnetic intensity map

Figure 15 demonstrate the total magnetic magnetic intensity map of the study area. From the qualitative trend analysis, it was deduced that; the area exhibits a complex and highly deformed geology arising from more than one tectonic generation. Structures trend mostly in NE and NNE directions. The interpreted north-east trends which occur mostly at the western and eastern flanks are representative of the observed geological contacts, sheared zones, granitic intrusions and quartz veins. A major north-south shear zone of about 1 km width related to the Kushaka-Kusheriki shear zone which traverses the eastern portion of the study area. The occurrence of primary gold and other sulfide mineralization in the area is observed to be the disseminated type within the vein quartz and quartzitic material.

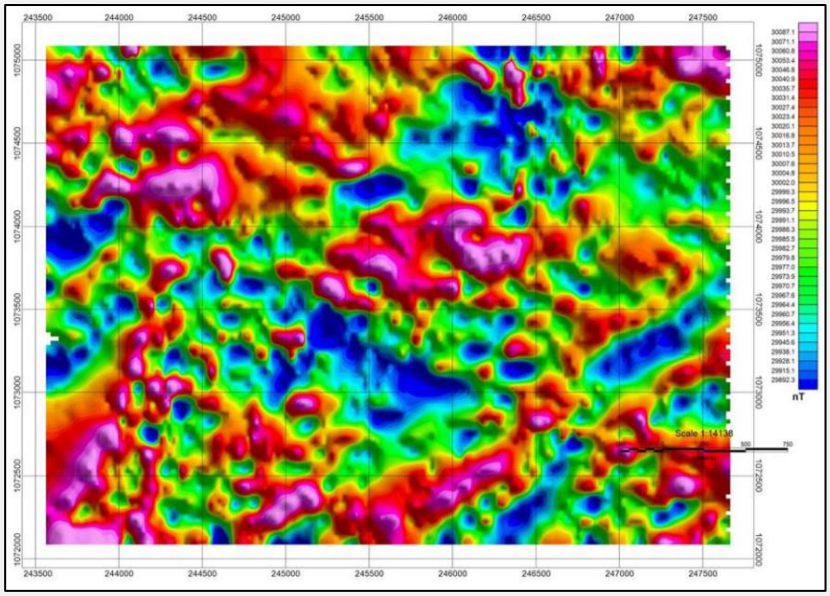

Figure 15. Total magnetic intensity map of the study area.

Second vertical derivative map

The second derivative filter was used to decreases broad and more regional anomalies. Thus, it has enhanced local magnetic responses which are interpreted as structures within the area. It emphasized the plan view boundaries of target zones (Especially intra-basement anomaly sources) as observed in the map.

Prominent magnetic lineaments are observed and marked by the red lines as seen in Figure 16. The areas which host most of the gold mineralization, generally trend in the northeast-southwest direction is depicted in the purple colour.

Figure 16 revealed the concentration of anomalous gold distribution in the study area. They are classified into three target areas marked as target A, B and C. Target A, B and C are the sections of the study area, having high anomalous gold concentrations. The gold anomaly legend is categorised with purple, brown, blue yellow and red colours in increasing order of concentration and they range from: 0.4 - 7.2; 7.3 - 16.4; 16.5 - 27.6; 27.7 - 61.7 and 61.8 - 201.0 respectively.

Relationship between interpreted lineaments in relation to gold mineralization demonstrates significant spatial correlation. This has established that the data used in the study has proven to be helpful in discovering identified and fresh geologic features in the area particularly when they are incorporated and the shape of magnetic signature acquired in the ground magnetic survey commonly suggests a step or an edge structures like dyke or intrusion, such structures of interest may hold mineralization at certain depth (Thompson, 1982; Silva et al., 2003).

Nearly all primary gold mineralization in the schist belts generally occur in quartz veins within different lithologies, consequently geophysical distinctiveness of the quartz veins becomes another important factors in prospecting and delineation gold deposit (Andongma et al., 2021).

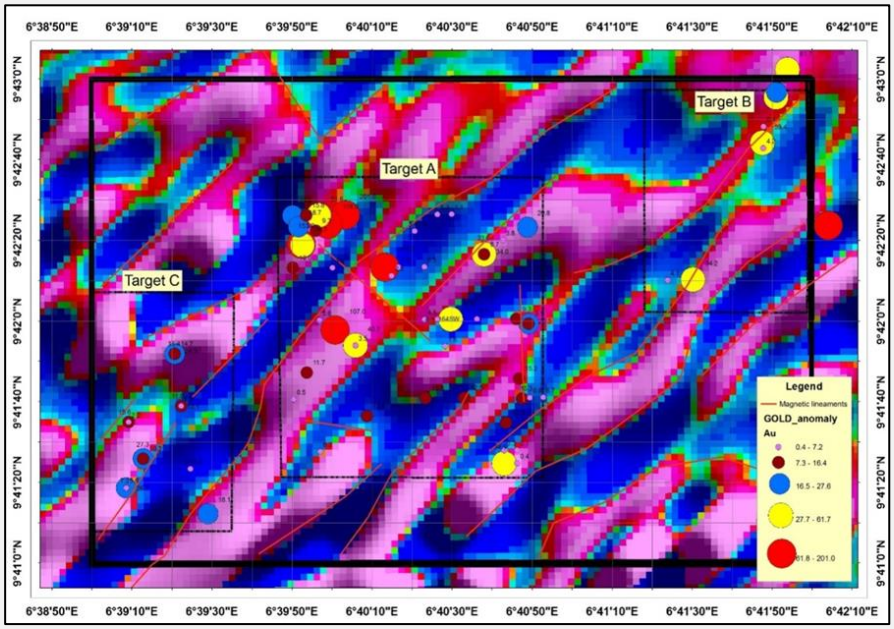

Figure 16. Anomalous gold sites plotted on the regional magnetic map of second vertical derivative.

Geochemical

Trace element geochemistry of gold bearing soils

The results of soils analysed with inductively coupled plasma/optical emission spectrometry (ICP/OES) for the concentration of gold and trace elements are presented in Table 2. Gold (Au) concentrations in the fractions of the heavy mineral, varied from <0.2 ppm to 201ppm with an average of 35.5 ppm. Obtained highest Au values were at locations GC15-29086, GC15-29088, GC15-29089 and GC15-29090 respectively (Table 2).

Almost all the soil samples investigated from different locations within the study area contains gold that exceeded the minimum value of gold in a geo-material (2000 ppb) that makes them to qualify as ores except UAPT23B and UARSI samples from GC15 – 29091, UAPT15A, UAPT15B, UAPT16A and UAPT16B from GC15-29090 and UAP8P09 from GC15-20989 (Guilbert & Park, 2007; Table 3).

Table 2. Trace elements concentration for the investigated soils of Owu area, Northcentral Nigeria

Location→	GC15-29086																
Elements→	Au	Cu	Pb	Zn	Ag	K	Ba	Sr	Ni	Co	Sc	Mo	W	Fe	Mn	Sb	Zr	K/Ba
Sample No.↓																		
UAPOP17	34.0	28.3	128.0	109.0	<2	0.09	38.0	20.8	20.0	16.0	20.0	7.0	13.0	13.1	6470.0	<5	296.0	0.002
UAP10P01	27.6	4.9	23.0	64.0	<2	0.03	27.0	4.3	15.0	10.0	18.5	<1	<10	15.0	10,000.0	<5	100.0	0.001
UAP10P02	15.8	9.9	38.0	64.0	<2	0.05	31.0	13.2	19.0	15.0	20.2	<1	<10	15.0	10,000.0	<5	356.0	0.002
UAP10P03	51.6	18.3	29.0	66.0	<2	0.06	35.0	10.6	24.0	18.0	12.5	<1	<10	11.6	4,810	<5	143.0	0.002
UAP10P05	201.0	19.6	43.0	67.0	<2	0.06	167.0	17.8	54.0	8.0	6.1	2	<10	6.8	4.210	<5	70.1	0
UAP10P17	3.3	28.8	33.0	57.0	<2	0.09	36.0	23.5	23.0	12.0	5.0	<1	<10	6.5	1,500	<5	43.1	0.03
Location→	GC15-29087																	
Elements→	Au	Cu	Pb	Zn	Ag	K	Ba	Sr	Ni	Co	Sc	Mo	W	Fe	Mn	Sb	Zr	K/Ba
Sample No.↓																		
UAP3P14	12.5	38.6	28.0	48.0	<2	0.07	37.0	22.7	32.0	45.0	5.5	22.7	<1	8.5	2,840.0	<5	98.4	0.002
UAP3P20	6.7	13.7	45.0	38.0	<2	0.09	35.0	19.8	14.0	7.0	10.8	19.8	1.0	9.8	3,300.0	<5	91.9	0.003
UAP6P03	5.6	15.9	20.0	20.0	<2	0.14	56.0	4.7	28.0	9.0	1.7	4.7	4.0	3.5	629.0	<5	26.1	0.003
UAP6P12	6.3	30.4	34.0	31.0	<2	0.09	66.0	13.0	31.0	12.0	5.7	13.0	<1	8.8	3000.0	<5	113.0	0.001
UAP6P13	33.8	407	53.0	24.0	<2	0.07	52.0	12.6	32.0	19.0	5.7	12.6	<1	9.6	2,990.0	<5	82.2	0.001
Location→	GC15-29088																	
Elements→	Au	Cu	Pb	Zn	Ag	K	Ba	Sr	Ni	Co	Sc	Mo	W	Fe	Mn	Sb	Zr	K/Ba
Sample No.↓																		
UAP8P01	10.0	18.2	23.0	132.0	<2	0.06	45.0	6.5	28.0	7.0	4.6	1.0	<10	5.7	2,710.0	<5	260.0	0.001
UAP8P08	110.0	20.9	31.0	187.0	<2	0.06	32.0	107.0	31.0	10.0	12.0	<1	18.0	8.0	5,900.0	<5	481.0	0.002
UAP8P09	1.3	17.2	20.0	39.0	<2	0.15	70.0	32.3	24.0	11.0	3.1	<1	<10	5.5	1,360.0	<5	81.2	0.002
Location→	GC15-29089																	
Elements→	Au	Cu	Pb	Zn	Ag	K	Ba	Sr	Ni	Co	Sc	Mo	W	Fe	Mn	Sb	Zr	K/Ba
Sample No.↓																		
UAPT15RV1	118.0	18.9	38.0	234.0	<2	0.05	54.0	38.1	37.0	44.0	13.1	<1	25.0	15.0	9,150.0	<5	66.9	0.0
UAPT18RV	20.8	19.6	50.0	83.0	<2	0.05	85.0	50.0	15.0	14.0	17.8	2.0	13.0	15.0	10,000.0	<5	40.9	0.0
UAPT22RV	15.2	29.6	37.0	100.0	<2	0.07	60.0	34.2	22.0	20.0	15.5	<1	<10	15.0	7,440.0	<5	44.5	0.001
UAPT24RV	15.3	40.2	64.0	197.0	<2	0.06	48.0	54.1	13.0	21.0	23.3	3.0	241.0	15.0	10,000.0	<5	483.0	0.001
UAP9RV1	34.3	23.8	41.0	255.0	<2	0.05	83.0	45.4	29.0	16.0	14.5	1.0	<10	11.8	9,340.0	<5	283.0	0
UAP9RV2	153.0	39.1	29.0	50.0	<2	0.08	232.0	35.5	39.0	26.0	8.0	3.0	<10	11.1	3,130.0	<5	46.8	0.0
USBS01	43.3	15.3	23.0	28.0	<2	0.81	262.0	27.2	17.0	4.0	4.2	2.0	<10	4.5	5,960.0	<5	352.0	0.003
USBSO6	61.7	12.7	18.0	17.0	<2	1.89	638.0	50.5	23.0	4.0	1.0	5.0	<10	3.9	3,020.0	<5	64.7	0.003
UBSE	59.4	20.3	10.0	20.0	<2	0.59	208.0	85.9	28.0	7.0	5.5	3.0	<10	5.8	4,800.0	<5	351.0	0.003
UBT1St.	4.2	37.2	33.0	56.0	<2	0.22	75.0	36.3	28.0	51.0	12.2	<1	21.0	9.5	10,000.0	<5	447.0	0.003
Location→	GC15-29090																	
Elements→	Au	Cu	Pb	Zn	Ag	K	Ba	Sr	Ni	Co	Sc	Mo	W	Fe	Mn	Sb	Zr	K/Ba
Sample No.↓																		
UAPT06B	107.0	39.20	38.0	108.0	<2	0.11	57.0	32.9	38.0	13.0	7.4	<1	<10	8.8	6,470.0	<5	239.0	0.002
UAPT15A	<2	24.0	68.0	61.0	<2	0.06	43.0	11.0	19.0	25.0	11.5	<1	<10	11.3	5,050.0	<5	575.0	0.001
UAPT15B	<2	25.8	46.0	38.0	<2	0.08	84.0	8.5	20.0	26.0	9.0	2.0	<10	11.4	2,900.0	<5	35.9	0.0
UAPT16A	<2	24.6	65.0	59.0	<2	0.11	63.0	12.0	35.0	12.0	5.2	<1	<10	7.0	4,290.0	<5	67.9	0.002

UAPT16B	<2	37.0	39.0	31.0	<2	0.10	45.0	7.9	24.0	16.0	4.8	<1	<10	7.3	2,770.0	<5	31.8	0.002
UAPT17A	34.0	30.8	32.0	108.0	<2	0.10	53.0	19.5	38.0	15.0	7.7	1	30.0	8.6	2,430.0	<5	125.0	0.002
Location→	GC15-29091																	
Elements→ Sample No.↓	Au	Cu	Pb	Zn	Ag	K	Ba	Sr	Ni	Co	Sc	Mo	W	Fe	Mn	Sb	Zr	K/Ba
UAPT23B	<0.2	71.6	100.0	314.0	<2	0.05	33.0	75.7	20.0	42.0	22.4	8.0	64.0	15.0	10,000.0	<5	367.0	0.002
UAPT26C	1.6	43.0	36.0	82.0	<2	0.1	53.0	20.1	37.0	12.0	6.4	2.0	<10	9.9	3,520.0	<5	55.5	0.002
UAPT27A	9.5	17.1	15.0	41.0	<2	0.08	70.0	6.7	15.0	6.0	4.6	1.0	<10	5.9	1,650.0	<5	33.3	0.001
UAPT27C	20.3	26.0	23.0	49.0	<2	0.09	110.0	6.6	18.0	16.0	8.0	3.0	<10	9.6	2,110.0	<5	40.6	0.0
UARS1	<0.2	20.9	49.0	82.0	<2	0.07	42.0	15.2	28.0	10.0	6.5	2.0	<10	8.0	3,810.0	<5	40.6	0.002
Location→	GC15-29093																	
Elements→ Sample No.↓	Au	Cu	Pb	Zn	Ag	K	Ba	Sr	Ni	Co	Sc	Mo	W	Fe	Mn	Sb	Zr	K/Ba
UCPT04A	16.4	31.5	18.0	49.0	<2	0.09	34.0	207.0	24.0	38.0	32.6	<1	<10	13.8	3,360.0	<5	16.3	0.003
UCPT04B	24.3	47.0	27.0	42.0	<2	0.12	67.0	91.1	26.0	57.0	17.4	<1	<10	13.6	1,670.0	<5	19.2	0.002
UCPT04C	14.7	35.3	27.0	71.0	<2	0.16	86.0	108.0	30.0	34.0	19.5	7	13.0	10.2	1,660.0	<5	30.2	0.002
UCPT08B	12.1	--	----	---	--	---	---	---	----	--	---	---	---	----	---	<5	--	----
UCPT08C	11.0	36.8	45.0	63.0	<2	0.05	31.0	64.2	20.0	28.0	12.8	<1	<10	11.8	3,420.0	<5	29.3	0.002
UCPT14A	15.6	20.0	67.0	141.0	<2	0.04	34.0	30.6	30.0	10.0	9.7	<1	<10	11.2	3,970.0	<5	85.7	0.001
UCPT15A	7.2	27.1	98.0	165.0	<2	0.05	39.0	139.0	11.0	28.0	28.9	<1	<10	15.0	10,000.0	<5	149.0	0.001
UCPT15B	26.7	27.3	102.0	151.0	<2	0.05	38.0	108.0	12.0	25.0	27.9	<1	<10	15.0	10,000.0	<5	269.0	0.001
UCPT15C	5.8	18.9	73.0	144.0	<2	0.09	45.0	171.0	11.0	19.0	26.9	<1	<10	15.0	8,710.0	<5	51.9	0.002

The gold content in the soil samples also exceeded its background values. This is a positive geochemical anomaly that indicates vertical or lateral proximity to higher grade of gold deposit. Reason being that financially viable rate of gold normally consists of very small quantity of dispersed gold. Even in the renowned ore of the Witwatersrand in South Africa, the normal concentration of gold is just about 16000 ppb (Craig & Vaughan, 1996).

The content of antimony (Sb) (<5 ppm) was relatively low in all the soils analysed. Antimony is recognized to be associated with gold deposits, and this low Sb value (<5 ppm) of Owu area may perhaps imply its distance to gold mineralization (Ashley et. al. 2003; Table 2).

Silver (Ag), a probable pathfinder element for Au, was characterized by very low values (<2 ppm) for all the investigated soil samples from different locations (Table 2). A likely rationale for this may possibly be due to co-precipitation alongside with Fe and Mn (Seewald & Seyfried, 1990). Further, intense weathering might also transport materials into the stream channels diluting Ag concentration (Wedepohl, 1995; Oke et al., 2014; Usman & Ibrahim, 2017). Some of the investigated soils are enriched in these two gold path finders; Mo (<1 – 19.8 ppm) and W (1 – 241 ppm) (Table 2).

The value of Zirconium (Zr) and Barium (Ba) is relatively low in the area of study (Table 2). Zr and Ba in the area are lower than the crustal abundances (Taylor & McLennan, 1995; Wedepohl, 1995; Table 4). The possible sources of these elements in the area is not clear, but heavy minerals like zircon and monazite are probable sources of Zr, while Ba was possibly will be contributed by feldspars or associated barite mineralization (Table 2).

Key et al. (2012) reported that the high content of Zr in stream sediments from Nigeria may possibly be as a result of severe tropical-chemical weathering, and constant physical weathering supported by wet season inundation and dry season winds, which efficiently separated most of the clay minerals, thus, leaving the sediments enriched in zircon and the other resistant, suggesting that, the anomalous concentrations of these elements are not related to the bedrocks. The enrichment of Zr is a strong indication of granitic source. This implies that the precursor for the sediments are of granitic origin. High content of Pb (10 – 128ppm; Table 2) with relatively regular distribution within the area of investigation fundamentally revealed the protolith from which the soil weathers from.

The nickel contents which ranged from 11 – 37ppm with an average of 25.16ppm was used to deduce the source of the mineralizing fluids for the protolith. The revealed average of nickel is an indication that the mineralizing fluids responsible for the protolith are of sedimentary-metamorphic origin (Barnes, 1997; Rye & Rye, 1974). Though, according to these authors, a 100ppm nickel concentration in samples suggests an igneous origin.

The composition of Co and Ni demonstrate comparable style of distribution within the area of investigation (Table 2). Nevertheless, most of the composition of Ni and Co in the investigated samples are lower than values required to term anomalies (Naseem et. al., 2012). Distribution of Ni and Co demonstrates a small spread. Such steadiness in sediments of different soils within the study area points toward regular environment of dispersion, uniform rock exposure, weathering pattern and climatic condition (Naseem et. al, 2012). This leads to virtually indistinguishable concentrations of Ni and Co in the soils; thus reflecting background dispersal (Table 2).

The K-Ba signatures of the mineralizing fluids were investigated for the studied soil samples (Tables 2 and 3), to infer the nature and control under which the gold was deposited (Danbatta et. al, 2008). The very low value in ratio of the lithophile elements (K/Ba = <0.01) for the investigated soil samples compared with average crustal ratio (K/Ba = 36) suggested that the Owu gold mineralization was not structurally controlled within the sediment/soil, but dispersed within the Owu soils (Kerrich, 1989).

Zn - Cu - Co - Pb was possibly related to sulphide mineralization which is probably connected with the felsic or granitic rock while the relationship between Ba, Sr, Co and Pb in abundance suggest occurrence of mafic and ultramafic rocks within the study area (Odokuma-Alonge & Adekoya, 2013).

Consequential direct comparative connection between elements; Au with Pb and Cu illustrate that Cu and Pb are marker elements for Au in the area under investigation (Fig. 17). Mobile elements Ni, Zn, Pb, As and Cu were utilized to trace concealed gold mineralization in Essase Concession, Eastern Region, Ghana (Amedjoe & Adjovu, 2013).

Table 3. Concentration of gold in the investigated soil samples of Owu area compared with acceptable background values

Location→ Elements→ Sample No.↓	GC15-29086 Au (ppm)	Au (ppb)	Crustal abundance of gold(ppb)	Clarke value (ppb)	Approximate minimum quantity to qualify as an ore (ppb)
UAPOP17	34.0	34,000	5	4	2000
UAP10P01	27.6	27,600	5	4	2000
UAP10P02	15.8	15,800	5	4	2000
UAP10P03	51.6	51,600	5	4	2000
UAP10P05	201.0	201,000	5	4	2000
UAP10P17	3.3	3,300	5	4	2000
Location→ Elements→ Sample No.↓	GC15-29087 Au				
UAP3P14	12.5	12,500	5	4	2000
UAP3P20	6.7	6,700	5	4	2000
UAP6P03	5.6	5,600	5	4	2000
UAP6P12	6.3	6,300	5	4	2000
UAP6P13	33.8	33,800	5	4	2000
Location→ Elements→ Sample No.↓	GC15-29088 Au				
UAP8P01	10.0	10,000	5	4	2000
UAP8P08	110.0	110,000	5	4	2000
UAP8P09	1.3	1,300	5	4	2000
Location→ Elements→	GC15-29089 Au				

Sample No.↓					
UAPT15RV1	118.0	118,000	5	4	2000
UAPT18RV	20.8	28,800	5	4	2000
UAPT22RV	15.2	15,200	5	4	2000
UAPT24RV	15.3	15,300	5	4	2000
UAP9RV1	34.3	34,300	5	4	2000
UAP9RV2	153.0	153,000	5	4	2000
USBS01	43.3	43,300	5	4	2000
USBSO6	61.7	61,700	5	4	2000
UBSE	59.4	59,400	5	4	2000
UBT1St.	4.2	4,200	5	4	2000
Location→	GC15-29090				
Elements→	Au				
Sample No.↓					
UAPT06B	107.0	107,000	5	4	2000
UAPT15A	<2	<2,000	5	4	2000
UAPT15B	<2	<2,000	5	4	2000
UAPT16A	<2	<2,000	5	4	2000
UAPT16B	<2	<2,000	5	4	2000
UAPT17A	34.0	34,000	5	4	2000
Location→	GC15-29091				
Elements→	Au				
Sample No.↓					
UAPT23B	<0.2	<200	5	4	2000
UAPT26C	1.6	1,600	5	4	2000
UAPT27A	9.5	9,500	5	4	2000
UAPT27C	20.3	20,300	5	4	2000
UARS1	<0.2	<200	5	4	2000
Location→	GC15-29093				
Elements→	Au				
Sample No.↓					
UCPT04A	16.4	16,400	5	4	2000
UCPT04B	24.3	24,300	5	4	2000
UCPT04C	14.7	14,700	5	4	2000
UCPT08B	12.1	12,100	5	4	2000
UCPT08C	11.0	11,000	5	4	2000
UCPT14A	15.6	15,600	5	4	2000
UCPT15A	7.2	7,200	5	4	2000
UCPT15B	26.7	26,700	5	4	2000
UCPT15C	5.8	5,800	5	4	2000

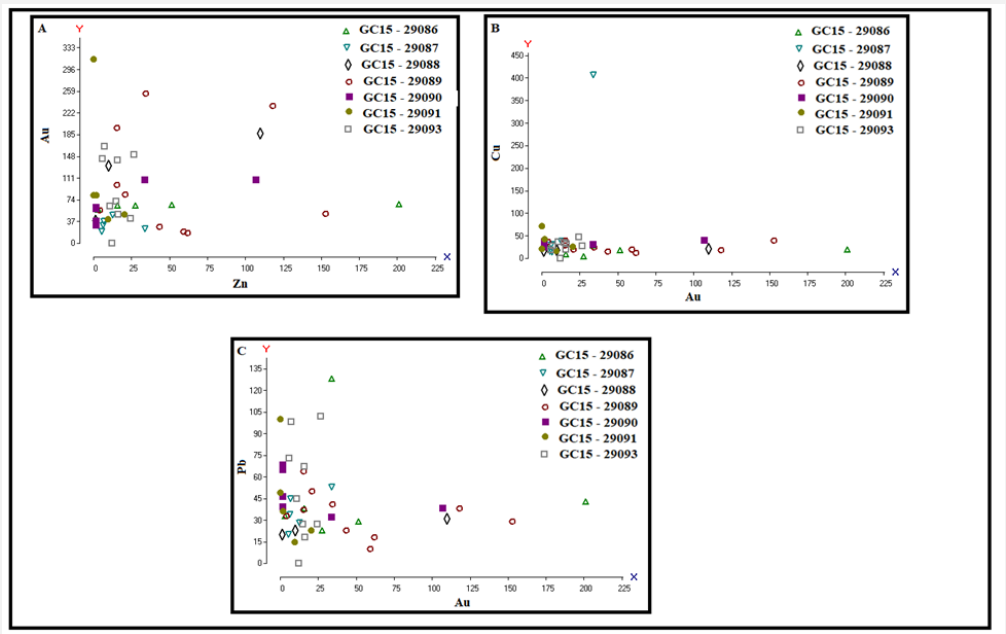

Figure 17. Bivariate plot of Au against Zn, Cu and Pb.

Enrichment Ratios

Element enrichment ratios (Albright, 2004) were designed to appraise the degree of enrichment and /or depletion of trace elements in the soils of the areas under investigation comparative to their crustal concentrations

The enrichment ratios are presented in Table 4. An ER = 1 signify that the soil is neither enriched nor depleted, > 1 or < 1 is an indication of enrichment or depletion of a known element relative to the average crustal contents.

The results illustrate that most of the elements (Sc, Ni, Sr, Zr and Ba) were generally low relative to their average crustal values, with mean ER <1.

Table 4. Summary of trace elements (ppm) in soils from Owu area, northcentral Nigeria, with published concentrations, soil guideline values for some potentially toxic elements and enrichment ratios, ER

Elements	This work n = 44	Upper Cont. crust		Soil		Sediments	Enrichment ratios, ER (n = 44)
		a	b	c	d	e	
Sc	12.0	11.0	16.0	---	----	---	0.8
Ni	25.16	20.0	56.0	19.0	22.0	16.9	0.4
Cu	35.63	25.0	25.0	25.0	22.0	16.5	1.4
Zn	88.03	71.0	65.0	60.0	66.0	41.0	1.4
Sr	44.2	350.0	333.0	----	----	201.0	0.1
Zr	151.9	190.0	203.0	----	-----	2,100	0.7
Mo	5.56	1.5	---	-----	---	0.73	3.7
Ba	81.37	550.0	584.0	----	----	808.0	0.1
Pb	43.23	20.0	15.0	19.0	30.0	28.0	2.9

a: Upper continental crust (Taylor and McLennan, 1995); b: Wedepohl, 1995; c: ICRCL/DEFRA Trigger concentrations for domestic gardens/allotments; d: US EPA soil guideline values; e: stream sediments from central Nigeria (Lapworth, 2012).

The composition of Mo is about 3.7 times its UCC value. Unlike Mo, the soil samples are only slightly enriched in Pb (2.9 times) while Cu and Zr (1.4 times), this suggest that artisanal mining conduct have not polluted the locality with these elements.

DISCUSSION

Based on the structural/geotectonics, geophysical and geochemical assessment of Kushaka-Kusheriki schist belt gold mineralization study; revealed positive correlation with other mineralized schist belts (Ilesha-ifewara, Maru, Anka,Kwaga, Birnin-Yauri, Okolom and Dogon-Daji) in Nigeria. The geotectonics regional fault system trend in the NE-SW and NNE-SSW (Okpoli et al., 2022). These different rock units: phyllites, gneisses, schists, quartzites, amphibolites and granitic intrusions, usually host the gold veins. Transcurrent and subsidiary fault systems are regional and local which typifies the Late Pan-African age (Ho & Greeves, 1987).

The deformation episodes witnessed in the study area like the NW-SE is typical of Kibaran orogeny (Okpoli & Oladunjoye, 2017) and Pan-African age. This deformation series evidenced in the Kushaka-Kusheriki schist belt made weathering, erosion and leaching of gold concentrates to be transported from higher gradients to lower gradients. The preponderance of the structural systems allowed alluvial system type of deposit and sulphide mineralization at depth in the study area (Andongoma et al., 2020)

The anomaly of gold was greater than the background values and it is significant to proximity to higher grade of gold deposit (Craig & Vaughan, 1996). Low amounts of Sb and Ag is due to co-precipitation of Fe and Mn and transportation distance of geo-materials in stream channels, thus diluting the Ag concentrations. The soils is greatly enriched with Mo and Ba, which serve as gold pathfinder (Ashley et al., 2003). Relatively low crustal abundance of Zr and Ba are due to Feldspathitic and granitic rocks as well as barite mineralization (Taylor a& McLenna, 1995; Wedepohl, 1995). Enrichment of Zr in the stream channel is caused by severe tropical weathering in Nigeria and is a precursor of granitic origin (Key et al., 2012). The Ni mineralizing fluids were adequate for protolith of sedimentary-metamorphic origin (Rye & Rye, 1974; Usman & Ibrahim, 2017) of the Nigerian schist belts. The Zn-Cu-Co-Pb were marker for sulphide mineralization and could be correlated to Ba, Sr, Cu, Pb abundance of mafic and

ultramafic rocks (Odokuma-Alonge & Adekoya, 2013). Au with Pb and Cu significantly indicate that Cu and Pb were marker elements for the Au in the schist belt (Amedjoe & Adjovu, 2013; Sanusi & Amigun, 2020). It is worth noting that this study holistically demonstrated the efficacy of employing integrated geotectonics, geophysical and geochemical approach in delineating gold deposit in Nigeria schist belts formation.

CONCLUSION

Primary gold mineralization localized in the quartz veins and its hydrothermal alterations with secondary gold mineralization as a result of weathering leading to alluvial and eluvial deposits were observed in the study area. Geological and geophysical mapping documented mainly the primary gold mineralization while the geochemical mapping of soil samples identified the secondary gold mineralization. The study area was zoned into three blocks: target A, B and C detailing the sampling targets used in the geological, geophysical and geochemical investigation. The main lithology in the Owu area under investigation comprises; mica schist, phyllite, amphibole and granitic gneiss with multiple quartz veins, suggesting an area of interest for gold occurrence. Structurally, the fold axes and quartz vein intrusions trend NE-SW parallel to the regional foliation of the rocks.

The primary gold occurrences are associated with intrusions on the quartz veins, schist and sheared zones while the secondary gold occurrences are associated with mechanical weathering processes resulting to paleo-(placers), alluvial deposits along stream channels.

From the magnetic and elevation maps, it was established that the region has undergone a distinct tectonic activity resulting in shearing and fracturing that showed a structurally controlled mineralization pattern consistent with the main magnetic trend of NE.

Almost all the soil samples qualified as ores as they contain gold that exceeded the minimum value of gold in a geo-material (2000 ppb) but the very low value in K/Ba (<0.01) for the investigated soil samples compared with average crustal ratio (K/Ba = 36) suggested that the secondary gold occurrences /Owu gold enrichment in the soil was not structurally controlled but dispersed within the soils as a result of mechanical weathering. Direct comparative connection between elements; Au with Pb and Cu indicated that Cu and Pb are marker elements for Au in the area and the enrichment factor indicated artisanal mining conduit have not polluted the locality with these (Mo, Pb, Cu, Zr Sc, Ni, Sr, Zr and Ba) elements.

ACKNOWLEDGEMENTS

The authors are grateful to the anonymous reviewers whose constructive comments have greatly improved this paper.

REFERENCES

Adeyi, A. A., & Babalola, B. A. (2017). Lead and cadmium levels in residential soils of Lagos and Ibadan, Nigeria. *Journal of Health and Pollution, 7*(13), 42-55. https://doi.org/10.5696/2156-9614-7-13.42

Ajakiaye, D. E., Hall, D. H., Ashiekaa, J. A., & Udensi, E. E. (1991). Magnetic anomalies in the Nigerian continental mass based on aeromagnetic surveys. *Tectonophysics, 192*(1-2), 211-230. https://doi.org/10.1016/0040-1951(91)90258-T

Ajibade, A. C. (1980). *Geotectonic evolution of the Zungeru region, Nigeria* (Doctoral dissertation, University College of Wales).

Albright, E. I. (2004). *Background concentrations of trace elements in soils and rocks of the Georgia Piedmont* (Doctoral dissertation, University of Georgia).

Amedjoe, C. G., & Adjovu, I. T. (2013). Application of the mobile metal ion geochemical technique in the location of buried gold mineralization in Essase Concession, Eastern Region. Ghana. *Journal of Geology and Mining Research, 5*(6), 147-160. https://doi.org/10.5897/JGMR2013.0175

Andongma, W. T., Gajere, J. N., Amuda, A. K., Edmond, R. R. D., Faisal, M., & Yusuf, Y. D. (2021). Mapping of hydrothermal alterations related to gold mineralization within parts of the Malumfashi Schist Belt, North-Western Nigeria. *The Egyptian Journal of Remote Sensing and Space Science, 24*(3), 401-417. https://doi.org/10.1016/j.ejrs.2020.11.001

Antweiler, J. C., & Campbell, W. L. (1982). Gold in exploration geochemistry. *Precious metals in the Northern Cordillera, 10*, 33-44.

Armstrong, M., & Rodeghiero, A. (2006). *Airborne geophysical techniques in Aziz*. Coal Operators' Conference, University of Wollongong and the Australasian Institute of Mining and Metallurgy, 113-131.

Arogundade, A. B., Awoyemi, M. O., Ajama, O. D., Falade, S. C., Hammed, O. S., Dasho, O. A., & Adenika, C. A. (2022). Integrated aeromagnetic and airborne radiometric data for mapping potential areas of mineralisation deposits in parts of Zamfara, North West Nigeria. Pure and Applied Geophysics, 179, 351–369. https://doi.org/10.1007/s00024-021-02913-w

Ashley, P. M., Craw, D., Graham, B. P., & Chappell, D. A. (2003). Environmental mobility of antimony around mesothermal stibnite deposits, New South Wales, Australia and southern New Zealand. *Journal of Geochemical Exploration, 77*(1), 1-14. https://doi.org/10.1016/S0375-6742(02)00251-0

Augie, A. I., Salako, K. A., Rafiu, A. A., & Jimoh, M. O. (2022). Geophysical magnetic data analyses of the geological structures with mineralization potentials over the southern part of Kebbi, NW Nigeria. *Mining Science, 29*, 179-203. https://doi.org/10.37190/msc222911

Barnes, H. L. (Ed.). (1997). *Geochemistry of hydrothermal ore deposits*. John Wiley & Sons.

Chouti, W. K., Adanve, M., & Mama, D. (2018). Dosage du plomb et du zinc dans les cultures de l'amarante (Amarantus cruentus) et de la Grande morelle (Solanum macrocarpum): cas de quelques sites maraîchers de Porto-Novo. *International Journal of Biological and Chemical Sciences, 12*(5), 2381-2395. https://doi.org/10.4314/ijbcs.v12i5.36

Clark, M. E., Archibald, N. J., & Hodgson, C. J. (1986). The structural and metamorphic setting of the Victory gold mine, Kambalda, Western Australia. In Proceedings of gold (Vol. 86, pp. 243-254).

Craig, J. R., Vaughan, D. J., & Hagni, R. D. (1994). *Ore microscopy and ore petrography* (Vol. 406). New York, NY: John Wiley & Sons.

Danbatta, U. A., Abubakar, Y. I., & Ibrahim, A. A. (2009). Geochemistry of gold deposits in Anka Schist Belt, Northwestern, Nigeria. *Nigerian Journal of Chemical Research, 14*, 19-29.

Darnley, A. G., Bjorklund, A., Bolviken, B., Gustavsson, N., Koval, P. V., Uk, J. P., ... & Xuejing, X. (1995). A global geochemical database. *Recommendations for international geochemical mapping. Final report of IGCP project, 259*.

Davies, R. S., Groves, D. I., Trench, A., & Dentith, M. (2020). Towards producing mineral resource-potential maps within a mineral systems framework, with emphasis on Australian orogenic gold systems. *Ore Geology Reviews, 119*, 103369. https://doi.org/10.1016/j.oregeorev.2020.103369

Garba, I. (2002). Late Pan-African tectonics and origin of gold mineralization and rare-metal pegmatities in the Kushaka schist belt, northwestern Nigeria. *Journal of mining and geology, 38*(1), 1-12. https://doi.org/10.4314/jmg.v38i1.18768

Gibert, D., & Galdeano, A. (1985). A computer program to perform transformations of gravimetric and aeromagnetic surveys. *Computers & Geosciences, 11*(5), 553-588. https://doi.org/10.1016/0098-3004(85)90086-X

Guilbert, J. M., & Park Jr, C. F. (2007). *The geology of ore deposits*. Waveland Press.

Ho, S. E., & Groves, D. I. (1987). *Recent advances in understanding Precambrian gold deposits*. Geology Department and University Extension, University of Western Australia Publication.

Kerrich, R. (1989). Archean gold: Relation to granulite formation or felsic intrusions?. *Geology, 17*(11), 1011-1015. https://doi.org/10.1130/0091-7613(1989)017%3C1011:AGRTGF%3E2.3.CO;2

Key, R. M., Johnson, C. C., Horstwood, M. S., Lapworth, D. J., Knights, K. V., Kemp, S. J., ... & Arisekola, T. (2012). Investigating high zircon concentrations in the fine fraction of stream sediments draining the Pan-African Dahomeyan Terrane in Nigeria. *Applied Geochemistry, 27*(8), 1525-1539. https://doi.org/10.1016/j.apgeochem.2012.04.009

Lapworth, D. J., Knights, K. V., Key, R. M., Johnson, C. C., Ayoade, E., Adekanmi, M. A., ... & Pitfield, P. E. (2012). Geochemical mapping using stream sediments in west-central Nigeria: Implications for environmental studies and mineral exploration in West Africa. *Applied Geochemistry, 27*(6), 1035-1052. https://doi.org/10.1016/j.apgeochem.2012.02.023

LeBoutillier, N. (2004). *The Baseline Lithogeochemistry of the Metasedimentary Rocks of Cornwall*. Unpublished Final Project Report.

Lu, Y., Song, S., Wang, R., Liu, Z., Meng, J., Sweetman, A. J., ... & Wang, T. (2015). Impacts of soil and water pollution on food safety and health risks in China. *Environment international, 77*, 5-15. https://doi.org/10.1016/j.envint.2014.12.010

Minty, B. R. S. (1991). Simple micro-levelling for aeromagnetic data. *Exploration Geophysics, 22*(4), 591-592. https://doi.org/10.1071/EG991591

Moon, C. J., Whateley, M. K. G., & Evans A. M. (2006). *Introduction of mineral exploration* (2nd ed.), Malden: Blackwell Publishing, 99p.

Naseem, S., Sheikh, S. A., Qadeeruddin, M., & Shirin, K. (2002). Geochemical stream sediment survey in Winder Valley, Balochistan, Pakistan. *Journal of Geochemical Exploration, 76*(1), 1-12. https://doi.org/10.1016/S0375-6742(02)00201-7

Obaje, N. G. (2009). *Geology and mineral resources of Nigeria* (Vol. 120, p. 221). Berlin: Springer.

Odokuma-Alonge, O., & Adekoya, J. A. (2013). factor analysis of stream sediment geochemical data from Onyami drainage system, Southwestern Nigeria. *International Journal of Geosciences, 4*(3), 656-661. http://dx.doi.org/10.4236/ijg.2013.43060

Oke, S. A., Abimbola, A. F., & Rammlmair, D. (2014). Mineralogical and geochemical characterization of gold bearing quartz veins and soils in parts of Maru Schist Belt Area, Northwestern Nigeria. *Journal of Geological research, 2014*(1), 314214. https://doi.org/10.1155/2014/314214

Okpoli, C. C., & Oladunjoye, M. A. (2017). Precambrian basement architecture and lineaments mapping of Ado-Ekiti region using aeromagnetic dataset. *Geosciences Research, 2*(1), 27-45. https://doi.org/10.22606/gr.2017.21005

Okpoli, C. C., Ogbole, J. O., Victor, O. A., & Okanlawon, G. O. (2022). Mineral exploration of Iwo-Apomu Southwestern Nigeria using aeromagnetic and remote sensing. *The Egyptian Journal of Remote Sensing and Space Science, 25*(2), 371-385. https://doi.org/10.1016/j.ejrs.2022.03.004

Okpoli, C. C., Olaniyan, O., Oyeshomo, A. V., & Chidi, P. (2024). Integrated geophysical characterization of Owu Gold mineralization part of Kushaka-Kusheriki Schist Belt, Northcentral Nigeria. *Geofísica Internacional, 63*(4), 1193-1207.

Oyediran, I. A., Nzolang, C., Mupenge, M. P., & Idakwo, S. O. (2020). Structural control and Sn-Ta-Nb mineralization potential of pegmatitic bodies in Numbi, South Kivu Eastern DR Congo. *Lithos, 368*, 105601. https://doi.org/10.1016/j.lithos.2020.105601

Oyeniyi, T. O., Salami, A. A., & Ojo, S. B. (2016). Magnetic surveying as an aid to geological mapping: A case study from Obafemi Awolowo University Campus in Ile-Ife, Southwest Nigeria. *Ife Journal of Science, 18*(2), 331-343.

Rahaman, M. A., Emofurieta, W. O., & Caen-Vachette, M. (1983). The potassic-granites of the Igbeti area: further evidence of the polycyclic evolution of the Pan-African belt in southwestern Nigeria. *Precambrian Research, 22*(1-2), 75-92. https://doi.org/10.1016/0301-9268(83)90059-1

Rasheed, A. I., & Abdulgafar, A. K. (2014). Impacts of artisanal mining on some heavy metals concentration in surface water in Kutcheri, Zamfara state north-western Nigeria. *Academic Journal of Interdisciplinary Studies, 3*(7), 74-82. http://dx.doi.org/10.5901/ajis.2014.v3n7p74

Reeves, C., Macnab, R., & Maschenkov, S. (1998). Compiling all the world's magnetic anomalies. Eos, *Transactions American Geophysical Union, 79*(28), 338-338. https://doi.org/10.1029/98EO00255

Rollinson, H. R. (2014). *Using geochemical data: evaluation, presentation, interpretation*. Routledge. https://doi.org/10.4324/9781315845548

Rye, D. M., & Rye, R. O. (1974). Homestake gold mine, South Dakota; I, Stable isotope studies. *Economic Geology, 69*(3), 293-317. https://doi.org/10.2113/gsecongeo.69.3.293

Salawu, N. B., Omosanya, K. O. L., Eluwole, A. B., Saleh, A., & Adebiyi, L. S. (2023). Structurally-controlled Gold Mineralization in the Southern Zuru Schist Belt NW Nigeria: Application of remote sensing and geophysical methods. *Journal of Applied Geophysics, 211*, 104969. https://doi.org/10.1016/j.jappgeo.2023.104969

Sanusi, S. O., & Amigun, J. O. (2020). Structural and hydrothermal alteration mapping related to orogenic gold mineralization in part of Kushaka schist belt, North-central Nigeria, using airborne magnetic and gamma-ray spectrometry data. *SN Applied Sciences, 2*, 1-26. https://doi.org/10.1007/s42452-020-03435-1

Scott, P. W., Reid, K. S., Shail, R. K., & Scrivener, R. C. (2003). Baseline geochemistry of Devonian low-grade metasedimentary rocks in Cornwall: preliminary data and environmental significance. *Geoscience in south-west England, 10*, 424-429.

Seewald, J. S., & Seyfried Jr, W. E. (1990). The effect of temperature on metal mobility in subseafloor hydrothermal systems: constraints from basalt alteration experiments. *Earth and Planetary Science Letters, 101*(2-4), 388-403. https://doi.org/10.1016/0012-821X(90)90168-W

Siegel, F. R. (1974). *Applied Geochemistry*. John Wiley & Sons, New Jersey.

Silva, A. M., Pires, A. C. B., Mccafferty, A., de Moraes, R. A. V., & Xia, H. (2003). Application of airborne geophysical data to mineral exploration in the uneven exposed terrains of the Rio Das Velhas greenstone belt. Brazilian Journal of Geology, 33(2), 17-28.

Skoog, D. A., West, D. M., Holler, F. J., & Crouch, S. R. (1996). *Fundamentals of analytical chemistry* (Vol. 33, pp. 53-55). Fort Worth: Saunders College Pub.

Smouni, A., Ater, M., Auguy, F., Laplaze, L., El Mzibri, M., Berhada, F., ... & Doumas, P. (2010). Évaluation de la contamination par les éléments-traces métalliques dans une zone minière du Maroc oriental. *Cahiers Agricultures, 19*(4), 273-279. https://dx.doi.org/10.1684/agr.2010.0413

Taylor, S. R., & McLennan, S. M. (1995). The geochemical evolution of the continental crust. *Reviews of geophysics, 33*(2), 241-265. https://doi.org/10.1029/95RG00262

Thompson, D. T. (1982). EULDPH: A new technique for making computer-assisted depth estimates from magnetic data. *Geophysics, 47*(1), 31-37. https://doi.org/10.1190/1.1441278

Usman, M. A., & Ibrahim, A. A. (2017). Petrography and geochemistry of rocks of Northern part of Wonaka Schist Belt, Northwestern Nigeria. *Nigerian Journal of Basic and Applied Sciences, 25*(2), 87-99. https://doi.org/10.4314/njbas.v25i2.10

Wedepohl, K. H. (1995). The composition of the continental crust. *Geochimica et cosmochimica Acta, 59*(7), 1217-1232. https://doi.org/10.1016/0016-7037(95)00038-2